Received: 17 August 2020 | Revised: 19 November 2020 | Accepted: 18 January 2021

DOI: 10.1111/bph.15390

RESEARCH PAPER

A plant-derived TRPV3 inhibitor suppresses pain and itch

Yalan Han[1,2] | Anna Luo[1,2] | Peter Muiruri Kamau[1,2,3] | Pitchayakarn Takomthong[4] | Jingmei Hu[5] | Chantana Boonyarat[4] | Lei Luo[1] | Ren Lai[1,3,6]

[1]Key Laboratory of Animal Models and Human Disease Mechanisms of Chinese Academy of Sciences/Key Laboratory of Bioactive Peptides of Yunnan Province, Kunming Institute of Zoology, Kunming, China

[2]University of Chinese Academy of Sciences, Beijing, China

[3]Sino-African Joint Research Center, Kunming Institute of Zoology, Chinese Academy of Sciences, Kunming, China

[4]Faculty of Pharmaceutical Sciences, Khon Kaen University, Khon Kaen, Thailand

[5]College of Life Sciences, Nanjing Agricultural University, Nanjing, China

[6]KIZ-CUHK Joint Laboratory of Bioresources and Molecular Research in Common Diseases, National Resource Center for Non-Human Primates, Kunming Primate Research Center and National Research Facility for Phenotypic & Genetic Analysis of Model Animals (Primate Facility), Institute of Zoology, Kunming, China

Correspondence
Chantana Boonyarat, Faculty of Pharmaceutical Sciences, Khon Kaen University, Khon Kaen, Thailand.
Email: chaboo@kku.ac.th

Lei Luo, Key Laboratory of Animal Models and Human Disease Mechanisms of Chinese Academy of Sciences/Key Laboratory of Bioactive Peptides of Yunnan Province, Kunming Institute of Zoology, Kunming, China.
Email: luolei@mail.kiz.ac.cn

Ren Lai, Sino-African Joint Research Center, Kunming Institute of Zoology, Chinese Academy of Sciences, Kunming, China.
Email: rlai@mail.kiz.ac.cn

Funding information
Chinese Academy of Sciences, Grant/Award Numbers: KC Wong Education Foundation, KFJ-STS-SCYD-304, XDB31000000, Youth Innovation Promotion Association, ZSTH-034, "Light of West China" Program; National Natural Science Foundation of China, Grant/Award Numbers: 21761142002, 31900332, 31930015; Science and Technology Department of Yunnan Province, Grant/Award Numbers: 2019-YT-053, 2019ZF003, 202001AT070121, 202001AW070015, 202003AD150008; the Ministry of Science and Technology of China, Grant/Award Number: 2018YFA0801403

Background and Purpose: Itching is the most frequent pathology in dermatology that has significant impacts on people's mental health and social life. Transient receptor potential vanilloid 3 (TRPV3) channel is a promising target for treating pruritus. However, few selecetive and potent antagonists have been reported. This study was designed to identify selective TRPV3 antagonist and elucidate its anti-pruritus pharmacology.

Experimental Approach: FlexStation and calcium fluorescence imaging were conducted to track the functional compounds. Whole-cell patch clamp was used to record itch-related ion channel currents. Homologous recombination and site-directed mutagenesis were employed to construct TRPV3 channel chimeras and point mutations for exploring pharmacological mechanism. Mouse models were used for *in vivo* anti-pruritus assay.

Key Results: An acridone alkaloid (citrusinine-II) was purified and characterized from *Atalantia monophylla*. It directly interacts with Y564 within S4 helix of TRPV3 to selectively inhibit the channel with a half maximal inhibitory concentration (IC_{50}) of 12.43 μM. Citrusinine-II showed potential efficacy to attenuate both chronic and acute itch. Intradermal administration of citrusinine-II (143 ng/skin site) nearly completely inhibited itch behaviours. It also shows significant analgesic effects. Little side effects of the compound are observed.

Conclusion and Implications: By acting as a selective and potent inhibitor of TRPV3 channel, citrusinine-II shows valuable therapeutic effects in pruritus animal models

Abbreviations: 2-APB, 2-aminoethoxydiphenyl borate; ASIC3, acid-sensing (proton-gated) ion channel 3; CCK8, cell counting kit-8; Na_v, voltage-gated sodium channel; TRP, transient receptor potential; TRPA1, transient receptor potential ankyrin 1; TRPM8, transient receptor potential melastatin 8; TRPV1, transient receptor potential vanilloid 1; TRPV2, transient receptor potential vanilloid 2; TRPV3, transient receptor potential vanilloid 3; TRPV4, transient receptor potential vanilloid 4.

Yalan Han, Anna Luo and Peter Muiruri Kamau contributed equally.

and is a promising candidate drug and/or lead molecule for the development of anti-pruritus drugs.

KEYWORDS
citrusinine-II, Inhibition, Itch, Pain, TRPV3

1 | INTRODUCTION

Itch, also known as pruritus, is the predominant symptom of skin that occurs in acute, chronic skin diseases and other disease such as neurologic, systemic and psychiatric diseases (Stander et al., 2007). Almost all human beings experience itch in the course of lifetime. Epidemiology survey showed that the prevalence of acute itch in the general population is 8.4% (Dalgard et al., 2004) and 13.5% for chronic itch (Matterne et al., 2011). Itch has a profound impact on quality of life as it affects sleep, social life and mental health, which leads to disorders such as anxiety, depression and insomnia (Silverberg, 2017). Furthermore, itch is a serious economic burden to the society due its high rate of therapeutic failure (Duque et al., 2004).

The cause of pruritus is extremely complicated and maybe caused by internal factors such as haematologic malignancy, renal failure, change of endocrine and metabolism, acquired immunodeficiency syndrome or external factors such as low humidity, inhaled substances, chemical materials and so forth (Song et al., 2018). Until now, the exact pathogenesis of pruritus remains unknown. Due to this poorly understood pathophysiology, the development of effective treatment modalities for pruritus has proven to be particularly difficult. However, recent advancements in pathophysiology of itch have identified new targets such as **transient receptor potential vanilloid (TRPV)** 1–4, **transient receptor potential ankyrin 1 (TRPA1)**, **transient receptor potential melastatin 8 (TRPM8)** and **voltage-gated sodium channel (Na_v)** 1.7–1.9 as therapeutic targets of this distressing symptom (Nattkemper et al., 2018).

Among all those newly identified targets, **TRPV3** channel is abundantly expressed in skin epidermal keratinocytes. Pharmaceutical and genetic studies have determined the crucial role of TRPV3 in the generation of itch (Spyra et al., 2017; Wang & Wang, 2017; Yamamoto-Kasai et al., 2012). From another angle, some chemical compounds from conventional medicines have been identified as TRPV3 blockers (Sun et al., 2018; Zhang et al., 2019), suggesting it is a potential target for itching treatment. Therefore it is rational to identify selective blockers of TRPV3 from potential medicinal herbs to treat itch.

By utilizing calcium florescent assay and electrophysiology, we identified **citrusinine-II**, an acridone alkaloid isolated from the medicinal plant *Atalantia monophylla* (L.) DC, as a potent and selective inhibitor of TRPV3 channel. Intradermal administration of citrusinine-II significantly attenuated itch behaviours. Our findings suggest a therapeutic potential for citrusinine-II in the treatment of pruritus and provide a pharmacological basis for this action.

What is already known

- TRPV3 channel is a promising target for treating a wide range of skin pathologies.

What this study adds

- Citrusinine-II selectively inhibits TRPV3 channel by binding to the S4 helix of TRPV3 (Y564).
- Citrusinine-II significantly attenuates itching and pain behaviours in mice models of these conditions.

What is the clinical significance

- The citrusinine-II binding site on TRPV3 might be a promising docking site for drug design.
- Citrusinine-II is a potential lead molecule for the development of anti-pruritus and analgesic drugs.

2 | METHODS

2.1 | Animals

All the animal experiments were performed following the Guide for the Care and Use of Laboratory Animals of Kunming Institute of Zoology, Chinese Academy of Sciences. All the animal experimental protocols in this study were approved by the Institutional Animal Care and Use Committees at Kunming Institute of Zoology, Chinese Academy of Sciences (Approval ID: SMKX-20190519-01). C57BL/6 male mice at age of 6–8 weeks (19–26 g) were purchased from the Laboratory Animal Research Center of Kunming Medical University, China. Mice were bred and housed in specific pathogen free conditions with controlled temperature (23 ± 2°C) and humidity (55 ± 5%) and 12-h light–dark cycle. Animals were maintained in groups of four per cage of 486 cm^2 × 15 cm depth with free access to water and standard food. During the experimental process, mice were anaesthetized through 100% CO_2 inhalation and killed by cervical dislocation. All mice were randomly assigned to different experimental groups and drugs (vehicle, citrusinine-II and morphine) were prepared and numbered by the designer. Data collection and conduction of all experiments were performed blindly. Animal studies are reported in

compliance with the ARRIVE guidelines (Percie du Sert et al., 2020) and with the recommendations made by the *British Journal of Pharmacology* (Lilley et al., 2020).

2.2 | Plant collection, extraction and isolation

The air-dried leaves of *A. monophylla* (16.0 kg) were identified and collected from Phuwieng District, Khon Kaen Province, Thailand. The leaves were air dried and ground into powder and extracted sequentially with hexane, ethyl acetate and methanol. The leachate was evaporated in vacuo to obtain dry extracts from hexane, ethyl acetate and methanol, respectively. After functional screening, the ethyl acetate portion was subjected to silica gel flash column chromatography and eluted with a gradient of hexane, ethyl acetate and methanol by gradually increasing the polarity. The eluates were collected every 50 ml and was separated using TLC, resulting in 10 fractions, F1–F10. F7 fraction was purified with silica gel flash column chromatography yielding F7.1–F7.4. Subfraction F7.2 was separated by Sephadex LH20 gel filtration eluting with methanol to yield citrusinine-II (1,3,5-trihydroxy-4-methoxy-10-methylacridone).

Natural product studies are reported in compliance with the recommendations made by the *British Journal of Pharmacology* (Izzo et al., 2020).

2.3 | Cell culture and transfection

HEK293T cells (RRID:CVCL_0063), CHO cells (RRID:CVCL_0213) and human keratinocytes cells (RRID:CVCL_0038) were cultured in DMEM supplemented with 10% FBS and 1% penicillin/streptomycin, kept at 37°C in an atmosphere with 95% O_2 and 5% CO_2 as previously described (Han et al., 2018; Luo et al., 2018). Cells were plated on 35-mm cell culture dish 24 h before transfection. Transient transfection was conducted by adding 4-μl Lipofectamine 2000 (Life technologies, USA), 4-μg channel cDNA and 1-μg EGFP cDNA into opti-MEM and then kept at room temperature for 15 min. DNA-Lipofectamine 2000 complexes was then added the cell culture dish. Electrophysiological experiments and fluorescence imaging assay were done 1–2 days after transfection. Mouse ***Trpv1***, mouse ***Trpv2***, mouse *Trpv3*, mouse ***Trpv4***, human *Trpa1*, mouse *Trpm8*, human *Scn9a* (gene for **$Na_v1.7$**) , mouse *Scn10a* (gene for **$Na_v1.8$**), human *P2rx3* and *Trpv3* mutant channels were transiently transfected using HEK293T cells while human ***ASIC3*** were transiently transfected using CHO cells.

2.4 | Isolation and culture of mouse keratinocytes

Newborn C57BL/6 mice (postnatal 3 days) were provided by the Laboratory Animal Research Center of Kunming Medical University, China. Skins dissected from WT postnatal mouse pups were pretreated with 75% ethanol for 100 s, washed with Ca^{2+}/Mg^{2+} free PBS and incubated with sterile 1.2 $U{\cdot}ml^{-1}$ dispase II (Roche, Switzerland) overnight (18 h) at 4°C. After mechanical dissociation and cleavage, epidermis were hatched with 0.1% collagenase I (Yuanye Bio-Technology Co., Ltd, China) for 45 min, which was then stopped with DMEM/F12 containing 10% FBS. Following filtration with 70- and 40-μm cell strainer and centrifugation at 400× *g* for 10 min, keratinocytes were collected and resuspended in Defined Keratinocyte Serum-Free Medium (Gibco, USA) containing 1% penicillin and streptomycin. Keratinocytes were grown in T25 cell culture flask and cultured in 37°C, 5% CO_2 incubator.

2.5 | Calcium assay using FlexStation

Intracellular calcium signal was measured by fluorescent calcium-sensitive dyes using the Calcium 5 assay kit in FlexStation 3 Microplate Reader (Molecular Devices, USA) (Luo et al., 2011). HBSS was used as the extracellular solution, which contained (in mM) 137 NaCl, 5.4 KCl, 0.1 Na_2HPO_4, 0.4 KH_2PO_4, 1.3 $CaCl_2$, 0.8 $MgSO_4$, 5.5 glucose, 4 $NaHCO_3$, 20 HEPES, pH = 7.4. HEK293T cells were seeded at a density of ~30,000 cells/well in 96-well black-walled plates (Thermo Scientific, USA) covered with poly-D-lysine. Cells were washed two times with HBSS and then loaded with loading solution containing dyes from the FLIPR Calcium 5 assay kit (Molecular Devices, USA) at 37°C for 1 h in the presence of 2-mM probenecid. After incubation, cells were washed with HBSS for three times and cell imaging was performed in HBSS. Fluorescence intensity at 525 nm was measured at an interval of 1.6 s, using an excitation wavelength at 494 nm and an emission wavelength at 525 nm.

2.6 | Calcium fluorescence imaging

HEK293T cells expressing mouse TRPV3 channels were incubated at room temperature for 45 min with 2-μM Fluo-4 AM (Invitrogen, USA) in Ringer's solution without 2-mM Ca^{2+} (140-mM NaCl, 2-mM $MgCl_2$, 2-mM $CaCl_2$, 10-mM glucose, 5-mM KCl and 10-mM HEPES, pH = 7.4). At the end of incubation, cells were washed twice with Ringer's solution. Normal Ringer's solution (with 2-mM Ca^{2+}) was used during imaging. Fluorescence images of HEK293T cells were acquired with an Olympus IX-81 microscope equipped with a Hamamatsu R2 charge-coupled device camera controlled by MetaFluor software (Molecular Devices, USA, RRID:SCR_014294). Fluo-4 was excited by a LED light source with a 500 ± 20 nm excitation filter, whereas fluorescence emission was detected with a 535 ± 30 nm emission filter. Change in fluorescence intensity, F, was normalized by the baseline fluorescence, F_0, in each cell and was expressed as $(F/F_0) \times 100\%$.

2.7 | Molecular biology and electrophysiological recordings

All chimeras (V1/3L and V1/3M) were constructed based on the mouse TRPV1 and mouse TRPV3 by the overlapping extension

method and confirmed by DNA sequencing, as previously described (Luo et al., 2019). Briefly, to generate V1/3L, the primer pairs (5′-GAA TACCTCGCCTGCCGAGGATTCCAGCAGATGGGC-3′ and 5′-GGTGA GGATGACATAATAGGCCAGTAACAGGATGAT-3′) for TRPV1 and primer pair (5′-CTGTTACTGGCCTATTATGTCATCCTCACCTTCGTC-3′ and 5′-CTGCTGGAATCCTCGGCAGGCGAGGTATTCTTTGTA-3′) for TRPV3. To generate V1/3M, the primer pairs (5′-GAATACC TCGCCTGCCGAGGATTCCAGCAGATGGGC-3′ and 5′-GTCGCCC AGGCCTATGATGGTGAACTTGAACAGCTC-3′) for TRPV1 and primer pair (5′-TTCAAGTTCACCATCATAGGCCTGGGCGACCTGAAC-3′ and 5′-CTGCTGGAATCCTCGGCAGGCGAGGTATTCTTTGTA-3′) for TRPV3. All the mouse TRPV3 single mutations were generated by using Fast Mutagenesis Kit V2, (SBS Genetech Co., Ltd., China) following the manufacturer's instruction and the mutations were confirmed by DNA sequencing.

All the experiments were performed with a HEKA EPC10 amplifier driven by PatchMaster software (HEKA Elektronik, Germany, RRID:SCR_00003) at room temperature. Microscopic currents were recorded under whole-cell configuration. For the TRP channel recording, both pipette solution and bath solution contained 3 HEPES, 130 NaCl and 0.2 EDTA (in mM, pH = 7.4). Cell membrane potential was held at 0 mV, the currents were elicited from +80 (300 ms) to −80 mV (300 ms) at 1-s intervals and the voltage ramps recording was elicited from −100 to +100 mV in 500 ms at 1-s intervals. For the sodium channels recording, the pipette solution contained 140 CsF, 1 EGTA, 10 NaCl, 3 KCl and 10 $MgCl_2$ (in mM, pH = 7.3). The bath solution contained 140 NaCl, 3 KCl, 1 $MgCl_2$, 1 $CaCl_2$ and 10 HEPES (in mM, pH = 7.3). Cell membrane potential was held at −80 mV. The currents were elicited with a testing pulse to −10 mV (100 ms) at 1-s intervals. For the ASIC3 channel recording, the pipette solution contained 10 NaCl, 140 KCl, 2 $CaCl_2$, 1 $MgCl_2$ and 10 HEPES (in mM, pH = 7.3). The bath solution contained 150 NaCl, 4 KCl, 1 $MgCl_2$, 2 $CaCl_2$ and 10 HEPES (in mM, pH = 7.3). The test solution contained 150 NaCl, 4 KCl, 1 $MgCl_2$, 2 $CaCl_2$ and 10 MES (in mM, pH = 5). Cell membrane potential was held at −60 mV. For the P2X3 channel recording, the pipette solution was 130 CsCl, 5 $MgCl_2$, 10 HEPES, 5 EGTA, 0.5 $CaCl_2$, 2 MgATP, 0.5 NaGTP and 5 KCl (in mM, pH = 7.2). The bath solution was 145 NaCl, 5 KCl, 2 $CaCl_2$, 1 $MgCl_2$, 10 D-glucose and 10 HEPES (in mM, pH = 7.4). Cell membrane potential was held at −70 mV.

2.8 | Isolation of mouse dorsal root ganglia neurons and current-clamp recordings

Eight-week-old C57BL/6 mice were killed through decapitation under CO_2 inhalation. The dorsal root ganglia neurons were quickly with great caution removed from the spinal cord and transferred into DMEM with 0.5 $g{\cdot}L^{-1}$ trypsin (Sigma-Aldrich, USA) and 1.0 $g{\cdot}L^{-1}$ collagenase (Sigma-Aldrich, USA) and incubated at 37°C for 30 min; 1.5 $g{\cdot}L^{-1}$ Trypsin inhibitor (Sigma-Aldrich, USA) was then added to cease enzymatic reaction. The dorsal root ganglia cells contained in 95% DMEM, 5% foetus-calf-serum were put into 35-mm dishes and incubated in 37°C for 3 h prior patch clamp recording. To record the membrane excitability of small-sized dorsal root ganglia neurons, the extracellular solution contained 140 NaCl, 3 KCl, 2 $CaCl_2$, 2 $MgCl_2$ and 10 HEPES (in mM, pH = 7.3) and the intracellular solution contained 140 KCl, 0.5 EGTA, 10 HEPES and 2 Mg-ATP (in mM, pH = 7.3). The recordings were acquired in a current-clamp mode and parameters related to action potential firing (amplitude and firing frequency). Action potentials were evoked by 1,000-ms depolarizing current pulses.

2.9 | Measurements of cell viability

Human keratinocytes cells or HEK293T cells were seeded into a 96-well plate at a density of 1×10^3 cells per well and incubated overnight at 37°C. Then, the cells were cultured in the medium, which dissolved different concentrations of citrusinine-II or 0.05% DMSO for 24 h. Ten microlitres of the cell counting kit-8 solution were added to each well (MedChemExpress, USA). After 30-min incubation at 37°C, the absorbance was measured at 450 nm.

2.10 | Molecular docking

RosettaDock (RRID:SCR_013393) application from Rosetta program suite version 2016.20 was used to dock citrusinine-II to mTRPV3 models (Xu et al., 2020). Citrusinine-II structure was downloaded from the PubChem compound NCBI component database (RRID: SCR_004284). The cryo-EM structure of the transmembrane domains of mouse TPRV3 (PDB: 6DVW) was downloaded from the Protein Data Bank (Singh et al., 2018). The cryo-EM structure model of mouse Trpv3 was relaxed in membrane environment by using Rosetta application and the lowest energy score were chosen for docking of citrusinine-II. A total of 10,000 models were generated for each docking trial and models were further scored with the binding energy between citrusinine-II and channel. Top 10 models with lowest binding energy (interface_delta_X) were identified as the candidates.

2.11 | Evaluation of scratching behaviour

To access the itch behaviour, the hair of C57BL/6 male mice (6–8 weeks) over the rostral area of the back was shaved using electric shaver 2 days before the start of experiments. Mice were then placed individually in an observation chamber (20 × 40 × 15 cm) at 25°C for 60 min before starting experiments. One bout of scratching behaviour was defined as the hind paws of mice touched or scratched the treated area until the behaviour stopped.

For acetone-ether-water test, the shaved area of mice was treated for 15 s by using a piece of cotton material soaked with mixed solution of acetone and diethylether (1:1), then immediately treated the same area for 30 s using the cotton soaked with distilled water. This treatment was done on daily basis for five consecutive

days. The vehicle control group was treated with water. On the sixth day, mice were put in the observation chamber 1 h prior experiments. For treatments, 50-μl DMSO (0.05%) or citrusinine-II were injected intradermally into mice shaved area. The mice scratching behaviours were recorded for 60 min following the injection of DMSO or citrusinine-II.

For locomotor activity test, the acetone-ether-water treated mice right neck were injected intradermally 50-μl saline containing 0.05% DMSO or citrusinine-II. The vehicle control group was treated with the same volume of DMSO (0.05%) dissolved in saline. Mice were then placed individually in an observation chamber and recorded for 60 min with an IR camera. The total distance of the mouse travelled in the observation chamber was determined as the locomotor activity.

For **histamine** test, the shaved area of mice was injected intradermally with 50-μl saline containing citrusinine-II 30 min before intradermal injection of 50-μl histamine (100 μM). The vehicle control group received the same volume of DMSO (0.05%) dissolved in saline. The scratching behaviours of mice were recorded for 30 min following histamine injection.

For **chloroquine** test, the shaving area of mice was injected intradermally with 50-μl saline containing citrusinine-II 30 min before intradermal injection of 50-μl saline containing chloroquine (400 μg). The vehicle control group received the same volume of DMSO (0.05%) dissolved in saline. The scratching behaviours of mice were recorded for 30 min following chloroquine injection.

2.12 | Histological analysis

The mice treated with acetone-ether-water for 5 days were killed via CO_2 inhalation followed by decapitation. The treated skin area of the mice was dissected, fixed in 4% formalin at 4°C overnight, dehydrated through an increasing concentration of ethanol and then embedded in paraffin. For histological analysis, thick sections (5 μm) were prepared and stained with haematoxylin and eosin. Stained sections were observed by light microscopy (Olympus, Japan).

2.13 | Blood brain barrier permeability assay

A 100-μl volume of 1-mM citrusinine-II dissolved in saline was injected into C57BL/6 male mice (8 weeks) via the tail vein. Mice were killed after 30 min. Brain samples were collected, suspended in 100% methanol (25 ml) at room temperature and homogenized after 3 h. The process was repeated three times. Brain samples were centrifuged at 5 000 g for 30 min and the supernatant were collected and lyophilized. The blood samples were also collected from the mice heart (500 μl) and immediately mixed with methanol (25 ml). The process of blood samples was the same as brain sample. The solvent-free brain and blood samples extracts were suspended in methanol and de-proteinized using a 3-kDa molecular filter (Millipore, USA). The filtrates after dry were re-suspended in methanol and analysed by LC–MS/MS detection (Exactive Plus, Thermo Scientific, USA). The immuno-related procedures used comply with the recommendations made by the *British Journal of Pharmacology*.

2.14 | Formalin-induced paw licking

Mice were injected intraperitoneally with 100-μl saline containing citrusinine-II or **morphine** 30 min before intraperitoneal injection of 20-μl 0.92% (vol/vol) formalin at the plantar surface of right hind paw. Mice were then placed individually in an observation chamber (20 × 40 × 15 cm). The time spent licking the injected paw was recorded during phase I (0–5 min post-injection) and phase II (15–30 min post-injection).

2.15 | Abdominal writhing induced by acetic acid

Mice were injected intraperitoneally with 100-μl saline containing citrusinine-II or morphine 30 min before intraperitoneal injection of 200-μl 0.8% (vol/vol) acetic acid, which induced abdominal contractions and hind limb stretching. The control group received the same volume of saline. Mice were placed in an observation chamber (20 × 40 × 15 cm) immediately after injection of acetic acid and abdominal constrictions were counted during 30 min.

2.16 | Hot plate test

A hot plate apparatus (HZ66-ZH-YLS-6B, China) was maintained at temperature of 53 ± 0.5°C and used to detect the pain in response to a thermal stimulus (Yang et al., 2013). Mice were injected intraperitoneally with 100-μl saline containing citrusinine-II or morphine 30 min before the thermal stimulus. The control group received the same volume of saline. The latency to the sign of hind paw licking or jumping to avoid heat nociception was taken as the index of the nociceptive threshold.

2.17 | Tail-flick test

A photothermal pain detector (YLS-12A; China) was used to test the pain threshold of mice (Wei et al., 2011). The light beam of the detector was focused on the middle portion of the tail. Mice were injected intraperitoneally with 100-μl saline containing citrusinine-II or morphine 30 min before photothermal heating of the tail. The control group was the same volume of saline. Tail withdrawal latency was measured as the time taken to withdraw the tail from the light beam.

2.18 | Statistics

The data and statistical analysis complied with the recommendations of the *British Journal of pharmacology* on experimental design and

analysis (Curtis et al., 2018). Studies were designed to generate groups in equal size. Sample sizes subjected to statistical analysis only if group size (n) ≥ 5 and the group size was the number of independent values. All data were expressed as the mean ± S.E.M. Statistical significance was assessed by one-way ANOVA with only one varying factor and two-way ANOVA with two varying factors for comparisons among three or more groups using Graphpad Prism 7 software (GraphPad Software Ltd., San Diego, CA, USA, RRID:SCR_002798). The post hoc tests (Bonferroni's or Sidak's tests) were conducted only if F in ANOVA achieved $P < .05$ and there was no significant variance inhomogeneity. $P < .05$ was considered significantly different. For data that did not pass normality testing, non-parametric statistics were used (Kruskal–Wallis followed by Dunn's post hoc test).

2.19 | Materials

Capsaicin, **allyl isothiocyanate**, **ruthenium red**, **2-APB**, ionomycin, **GSK1016790A** and **menthol** were purchased from Sigma-Aldrich (USA). **Carvacrol** was purchased from Macklin (China). Formalin was purchased from Macklin (China). ATP was purchased from Sigma-Aldrich (USA). Friedelin was purified from Atalantia monophylla (L.) DC. These compounds were dissolved in DMSO to make 100-mM stock solutions. For electrophysiological experiments and fluorescence imaging assay, the stock solutions were diluted in bath solution to acquire the working concentrations. **Histamine** was purchase from MedChemExpress (USA), which was dissolved in DMSO to 100 mM. Morphine was purchased from Shenyang First Pharmaceutical Co., LTD (China) while acetic acid glacial and chloroquine diphosphate salt were purchased from Sigma-Aldrich (USA). All four of these compounds required for animal experiments were diluted in saline to make the desired concentrations.

2.20 | Nomenclature of targets and ligands

Key protein targets and ligands in this article are hyperlinked to corresponding entries in the IUPHAR/BPS Guide to PHARMACOLOGY http://www.guidetopharmacology.org and are permanently archived in the Concise Guide to PHARMACOLOGY 2019/20 (Alexander et al., 2019).

3 | RESULTS

3.1 | Citrusinine-II is an antagonist of TRPV3 channel

To identify selective and potential TRPV3 channel inhibitors, we focused on *Atalantia monophylla* (L.) DC, a traditional anti-pruritus herb medicine (Figure 1a). Following its ethanolic extraction, further purification was done where a total of 10 compounds were isolated, including citrusinine-II (Figure S1 and Table S1). The ethanolic extracts and purified compounds were functionally tested on the TRPV3 channels by FlexStation calcium assay. As shown in Figure 1b, 2-aminoethoxydiphenyl borate (2-APB) potently increased calcium signals in HEK293T cells transiently transfected with mouse TRPV3 channels. Similar to a non-selective inhibitor (ruthenium red, 50 μM) of TRPV3 channel, ethanol extract of *A. monophylla* (10 mg·ml^{-1}) and citrusinine-II (10 μM) significantly inhibited the 2-APB-elicited calcium signals, with inhibition percentage 23.17 ± 1.63 and 47.16 ± 4.17, respectively (Figure 1c). These results indicate that citrusinine-II is a novel antagonist of TRPV3 channel.

3.2 | Inhibitory properties of citrusinine-II

To further confirm the inhibitory effect of citrusinine-II on TRPV3 channel, we used calcium imaging technique to detect the intracellular fluorescent calcium level (Figure S2a–c). Friedelin, a triterpene compound isolated from *A. monophylla*, had no inhibitory effect on TRPV3 channel and was used as negative control. When 2-APB was pretreated with 50-μM friedelin, it elicited a significant fluorescent calcium signal (Figure S2b). However, pretreatment with 50-μM citrusinine-II almost completely inhibited the 2-APB elicited calcium signal without disturbing ionomycin responses (Figure S2c). These calcium imaging assays further suggest that citrusinine-II efficiently antagonized the 2-APB-evoked TRPV3 activation.

Whole-cell patch clamp recordings were performed on both HEK293T cells heterologously expressing TRPV3 channel and mouse primary cultured keratinocytes. Perfusion of 50-μM citrusinine-II almost completely inhibited the TRPV3 channel currents evoked by 200-μM 2-APB (Figure 1d). A similar inhibitory effect was obtained by voltage ramp recordings (Figure 1e). In addition, the dose-dependent inhibition data of citrusinine-II on TRPV3 were fitted to Hill equation yielding an IC_{50} value of 12.43 ± 1.86 μM (n = 6) and a Hill coefficient of 1.05 (Figure 1f). Since TRPV3 channel is abundantly expressed in epidermal keratinocytes, we further investigated the inhibitory effect of citrusinine-II on endogenous TRPV3. Primary epidermal keratinocytes were isolated from the skin of newborn C57BL/6 mice (Figure 1g). Application of TRPV3 agonist cocktail (200-μM 2-APB + 500-μM carvacrol) on keratinocytes elicited TRPV3-like currents and 50-μM citrusinine-II almost completely inhibited the currents (Figure 1h). The voltage ramp recordings showed similar inhibitory effect of citrusinine-II (Figure 1i). These results further confirm that citrusinine-II is an inhibitor of native TRPV3 channel.

3.3 | High selectivity of citrusinine-II on TRPV3 channel

After confirming the inhibitory effect of citrusinine-II on TRPV3 channel we investigated its selectivity on other itch-related ion channels. TRPV1, TRPV4, TRPA1 and TRPM8 channels have been reported to be involved in itch signalling (Nattkemper et al., 2018) and the currents of these channels were recorded by a voltage ramp from −100

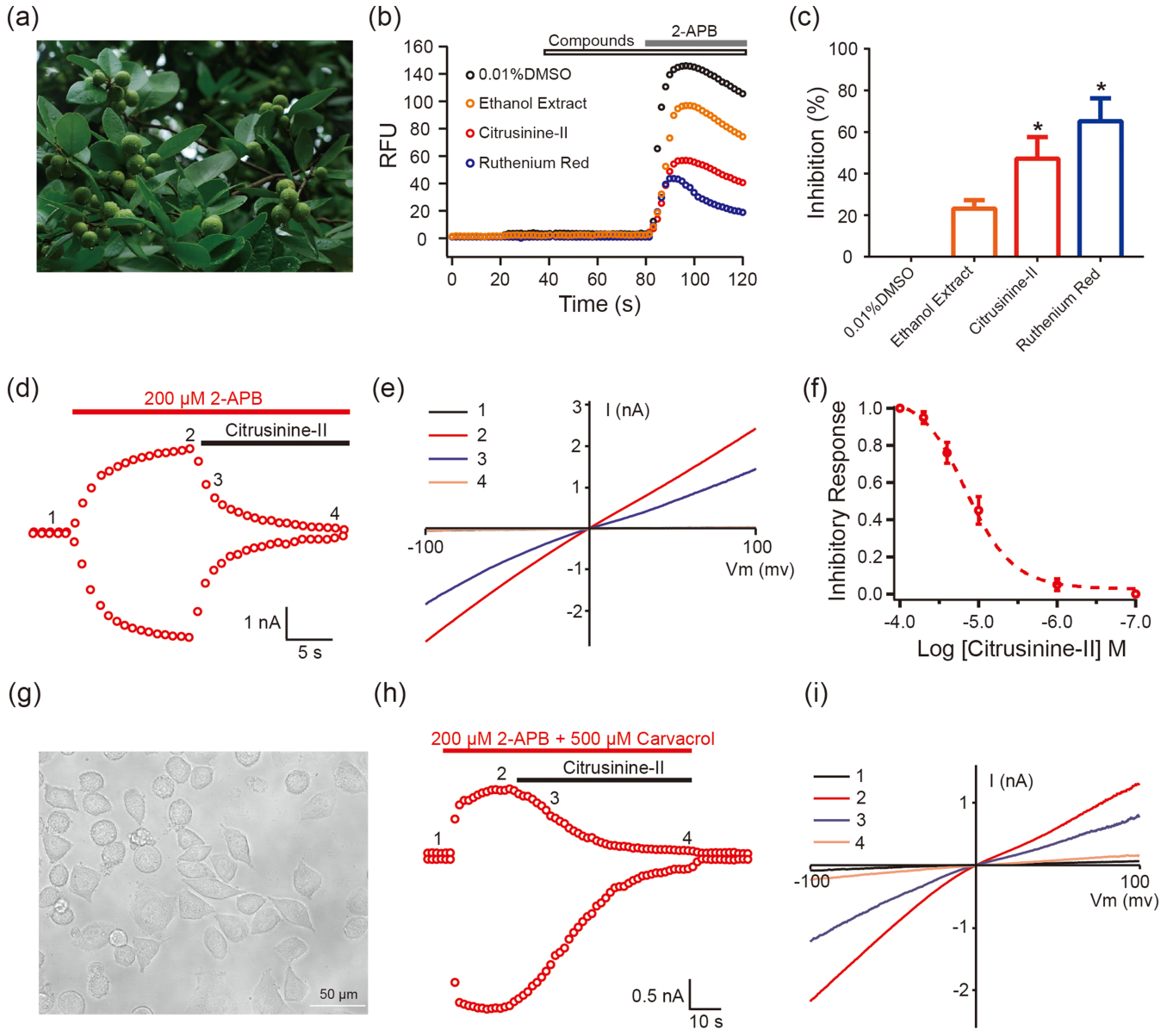

FIGURE 1 Identification of citrusinine-II as a potent inhibitor for TRPV3 channels. (a) Representative photograph of *Atalantia monophylla* (L.) DC, from which citrusinine-II was isolated. (b) Inhibition of TRPV3 channel expressed in HEK293T cells in response to 0.01% DMSO, 10 mg·ml^{-1} ethanol extract of *A. monophylla*, 10-μM citrusinine-II and 50-μM ruthenium red mixed with 200-μM 2-APB in FlexStation calcium fluorescent assay. (c) A summary for inhibition of intracellular fluorescent Ca^{2+} from panel (b). Asterisks denote statistical significance using Kruskal–Wallis followed by Dunn's post hoc test. (d) Whole-cell patch clamp recordings of TRPV3 currents in response to 2-APB alone (200 μM, red bar) or co-application of 50-μM citrusinine-II (black bar). (e) Current–voltage curves of TRPV3 in response to voltage ramps from −100 to +100 mV before (1) and after 200-μM 2-APB (2) and co-application of 200-μM 2-APB and 50-μM citrusinine-II (3) and washout (4). (f) Hill equation fitting of dose-dependent inhibition of 2-APB-mediated TRPV3 activation by citrusinine-II with an IC_{50} of 12.43 ± 1.86 μM (n = 6), Hill slope, 1.05. Data are presented as the mean ± S.E.M. (g) Representative photograph of primary epidermal keratinocytes which is isolated from mouse skin. (h) Whole-cell patch clamp recordings of primary mouse epidermal keratinocyte currents in response to 200-μM 2-APB and 500-μM carvacrol (red bar) or co-application of 50 μM citrusinine-II (black bar). (i) Current–voltage curves of primary mouse epidermal keratinocyte in response to voltage ramps from −100 to +100 mV before (1) and after 200-μM 2-APB and 500-μM carvacrol (2) and co-application of 200-μM 2-APB, 500-μM carvacrol and 50-μM citrusinine-II (3) and washout (4)

to +100 mV for 500 ms. Perfusion of 50-μM citrusinine-II on TRPV1 currents elicited by 10-μM capsaicin had a slight reduction of about 5.4 ± 1.3% (Figure 2a) or about 3.6 ± 1.1% of TRPA1 current induced by 200-μM allyl isothiocyanate (Figure 2b) or no inhibitory effect of TRPV4 current activated by 100-nM GSK1016790A (Figure 2c), as compared with complete inhibition of TRPV3 channel (Figure 1d,e). TRPM8 channel agonists, such as **icilin** and **menthoxypropanediol (colling agent 10)** have shown good anti-itching effects (Han

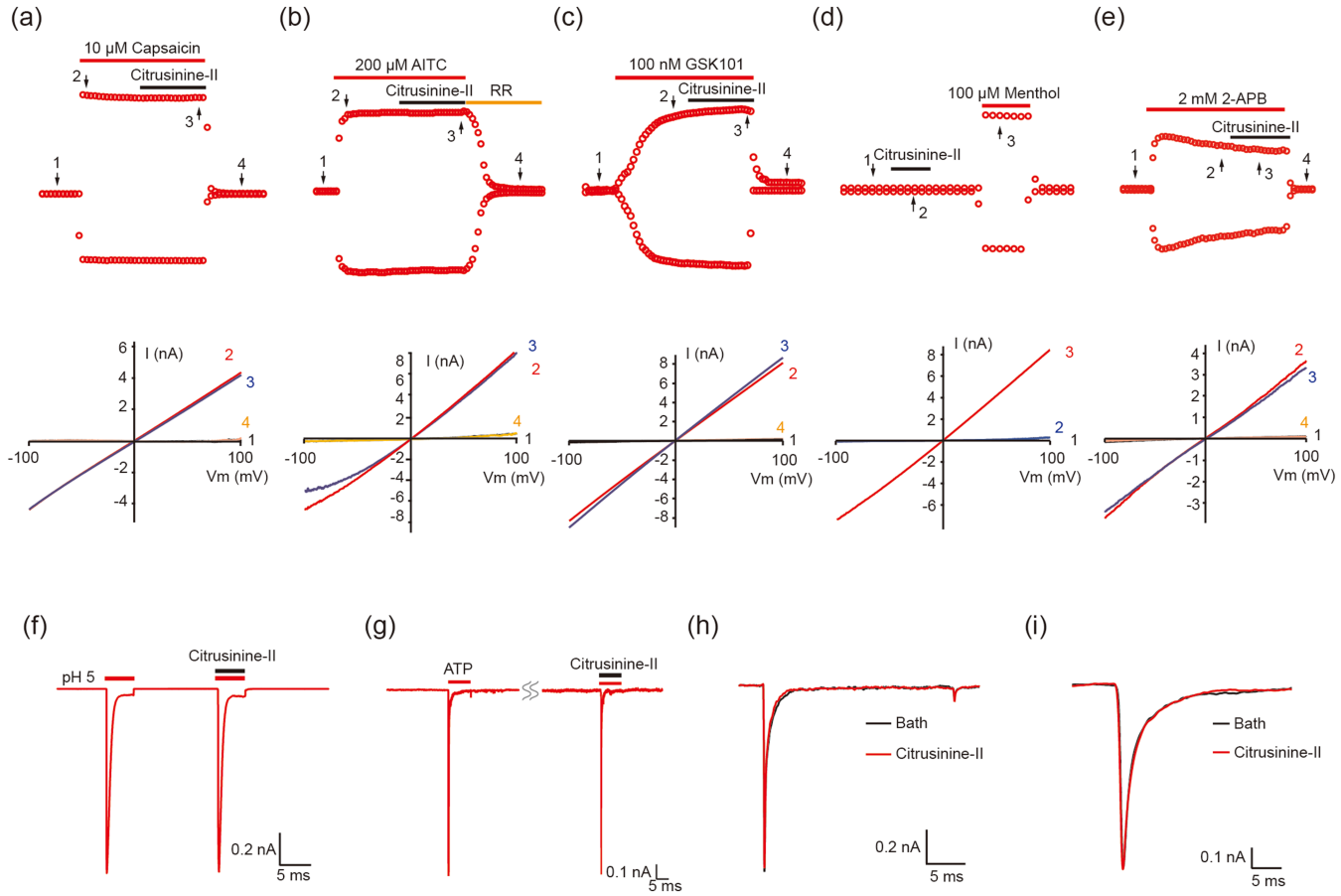

FIGURE 2 Selective inhibition of TRPV3 channel by citrusinine-II. (a) Representative mouse TRPV1 current activated by 10-μM capsaicin (red bar) before and after its co-application with 50-μM citrusinine-II (black bar) and washout. Lower panel: Current–voltage curves of TRPV1 in response to voltage ramps from −100 to +100 mV before (1) and after 10-μM capsaicin (2) and co-application of 10-μM capsaicin and 50-μM citrusinine-II (3) and washout (4). (b) Representative human TRPA1 current activated by 200-μM allyl isothiocyanate (AITC; red bar) or in the presence of 50-μM citrusinine-II (black bar) and completely inhibited by 20-μM ruthenium red (RR, yellow bar); lower panel: current–voltage curves of TRPA1 in response to voltage ramps from −100 to +100 mV before (1) and after 200-μM AITC (2), and co-addition of 200-μM AITC and 50-μM citrusinine-II (3) and total inhibition by ruthenium red (4). (c) Representative mouse TRPV4 current elicited by 100-nM GSK1016790A (GSK101; red bar), before and after its co-application with 50-μM citrusinine-II (black bar) and washout. Lower panel: current–voltage curves of TRPV4 in response to voltage ramps from −100 to +100 mV before (1) and after 100-nM GSK101 (2), and co-application of 100-nM GSK101 and 50-μM citrusinine-II (3) and washout (4). (d) Representative mouse TRPM8 whole-cell current in response to 50-μM citrusinine-II (black bar) and 100-μM menthol (red bar) and washout. Lower panel: current–voltage curves of TRPM8 in response to voltage ramps from −100 to +100 mV in response to 50-μM citrusinine-II (1), 100-μM menthol (2) and washout (3). (e) Representative mouse TRPV2 current activated by 2-mM 2-APB (red bar) before and after its co-application with 50-μM citrusinine-II (black bar) and washout. Lower panel: current–voltage curves of TRPV2 in response to voltage ramps from −100 to +100 mV before (1) and after 2-mM 2-APB (2), and co-addition of 2-mM 2-APB and 50-μM citrusinine-II (3) and washout (4). (f) Whole-cell currents recorded from CHO cells expressing human ASIC3 in response to pH 5 and a mixture of pH 5 and 50-μM citrusinine-II. (g) Representative human P2X3 receptor current activated by 300 μM ATP and its co-application with 50-μM citrusinine-II. Representative whole-cell human $Na_v1.7$ (h) and mouse $Na_v1.8$ (i) currents recorded in the absence or presence of 50-μM citrusinine-II

et al., 2012; Misery et al., 2019). Thus, citrusinine-II was also checked on TRPM8 channel (Figure 2d), however no discernible activity was found. Considering that 2-APB is a common activator of TRPV1, TRPV2 and TRPV3 channels (Colton & Zhu, 2007), we tested the inhibitory activity of citrusinine-II on TRPV2. After excluding the effect of channel desensitization, 50-μM citrusinine-II showed no significant inhibition of TRPV2 (Figure 2e). In addition, other ion channels such as ASIC3, P2X3, $Na_v1.7$ and $Na_v1.8$ channels have been reported to play role in itching (Devigili et al., 2014; Kuhn et al., 2020; Peng et al., 2015; Shiratori-Hayashi et al., 2019). Application of 50-μM citrusinine-II on these channels had no obvious activity (Figure 2f–i). These results indicate that citrusinine-II is a highly selective antagonist of TRPV3 channel. We also investigated the cytotoxicity of citrusinine-II *in vitro* using CCK8 assay. Human keratinocytes is one kind of human skin cell lines that natively expresses TRPV3 channels. Compared to the 0.05% DMSO group, citrusinine-II showed no

notable cytotoxicity on human keratinocytes cells (Figure S3a). The cytotoxicity against normal HEK293T cells was also investigated. Citrusinine-II showed no striking cytotoxicity on HEK293T cells (Figure S3b). These results suggest that citrusinine-II is a safe molecule *in vitro*.

3.4 | S4 helix of TRPV3 channel is related to the inhibition of citrusinine-II

Considering that citrusinine-II selectively inhibits TRPV3 channel, we sought to understand the molecular interactions between citrusinine-II and TRPV3. Since TRPV1 is almost insensitive to citrusinine-II, several chimeras were constructed by homologous substitution between TRPV3 and TRPV1 (Figure 3a). Previous reports have proved that pore region of TRPV3 channel is associated with either chemical or thermal stimuli (Chung et al., 2005; Grandl et al., 2008). Therefore, chimeras were primarily constructed within the pore domain. Of interest, we found that $V_{1/3}L$ chimera (Figure 3a) containing Leu^{551}-Thr^{660} segment of TRPV3 was inhibited in the presence of citrusinine-II. More specifically, $V_{1/3}M$ chimera containing Leu^{551}-Thr^{636} part of TRPV3 was also sensitive to citrusinine-II. These results suggested that site/sites located in the Leu^{551}-Thr^{636} region of TRPV3 play a role in the inhibitory effect of citrusinine-II.

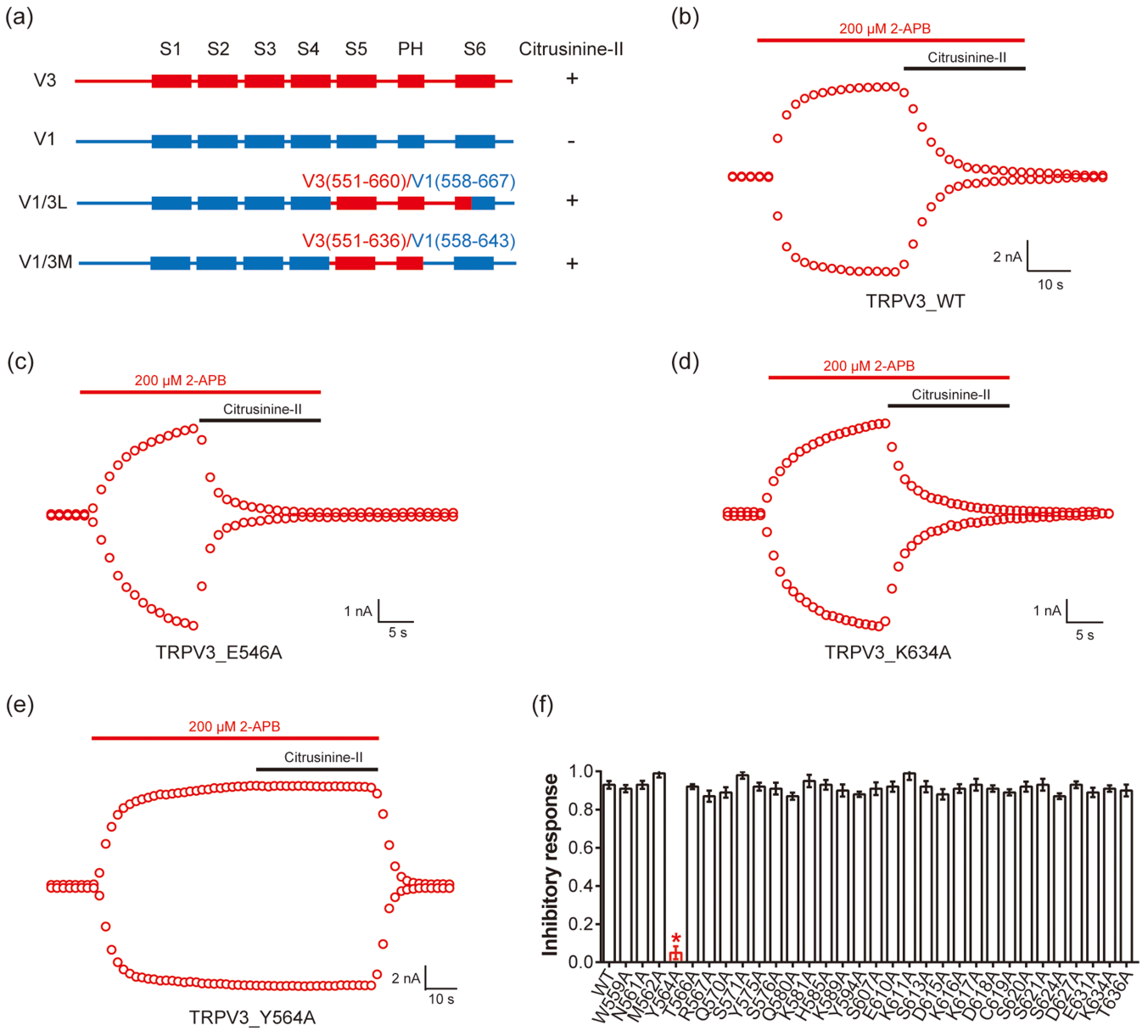

FIGURE 3 Citrusinine-II targets Y564 in S4 transmembrane helix. (a) Responsiveness to citrusinine-II by chimeric channels between mTRPV1 (V1, blue) and mTRPV3 (V3, red). (b–e) Representative whole-cell current response of point mutants to 200-μM 2-APB and co-application of 200-μM 2-APB and 50-μM citrusinine-II. (f) Comparison of citrusinine-II inhibitory response in mTRPV3 wild type (WT) and point mutants (n = 5, *P < .05, significantly different from WT; one-way ANOVA followed by Bonferroni's post hoc test)

These findings triggered our interest to conduct point-mutation screenings of the Leu^{551}-Thr^{636} region of wild-type TRPV3 channel (Figure 3b–f). Functional screening of the mutants for the chimera region identified Y564 located in the S4 helix as a key residue for the citrusinine-II-induced channel inhibition (Figure 3e). An alanine substitution (Y564A) at this site remarkably reduced the binding affinity of citrusinine-II (Figure 3f). Rosetta modelling between TRPV3 channel and citrusinine-II shows that Y564 in TRPV3 channel directly interact with benzene ring of citrusinine-II via π–π stacking interaction (Figure S4). These results indicate that Y564 within the transmembrane region of S4 helix is essential for the inhibitor action of citrusinine-II.

3.5 | Citrusinine-II attenuates pruritic scratching behaviour

Since TRPV3 channel plays a crucial role in pruritus pathology and that citrusinine-II has a potent inhibitory effect on TRPV3 channel, we tested the anti-pruritus activity of citrusinine-II. Acetone-ether-water-induced dry skin mouse model was constructed by daily treatment of mouse's nape skin with acetone/ether (1:1) mixture and distilled water resulting to a spontaneous scratching behaviour, which was thought to be histamine-independent. Following five consecutive days treatment, the acetone-ether-water-treated nape of mouse developed skin dryness as compared with vehicle control of water treatment (Figure 4a,b). As a hallmark of psoriatic chronic itch in humans, the mouse skin epidermal thickening was checked. Haematoxylin–eosin staining of nape sections revealed that mice treated with acetone-ether-water developed an epidermal hyperplasia with infiltration of inflammatory cells as compared with vehicle group (Figure 4c,d). On the sixth day, the C57BL/6 mice were allowed to acclimatize at room temperature for 60 min and then intradermal injection on the nape was performed using 0.05% DMSO as vehicle and different concentrations of citrusinine-II (5 and 10 μM in 50 μl/site equivalent to 71.5 and 143 ng/site, respectively). The itch scratching behaviour was recorded using a video camera for 60 min following the injection of vehicle and citrusinine-II. As shown in Figure 4e, acetone-ether-water-DMSO treatment significantly and remarkably increased the spontaneous scratching behaviour bouts with a number of 63.6 ± 4.6 compared with vehicle-DMSO treatment group at 5.0 ± 0.6. On the contrary, 5- and 10-μM citrusinine-II treatment dose-dependently and significantly decreased the spontaneous scratching behaviour with a number of 42.0 ± 4.7 and 17.6 ± 1.0, respectively, indicating that citrusinine-II suppresses acetone-ether-water-induced scratching behaviour. To investigate the possibility of any side effects *in vivo* caused by citrusinine-II treatment, we also measured the spontaneous locomotor activity and no adverse effects evoked by citrusinine-II injection were noted. After intradermal treatment with vehicle (0.05% DMSO) and citrusinine-II (5 and 10 μM, 50 μl/site) into the nape, the locomotor travel distance within 60 min was detected and no significant alternation was found (Figure S3c). Moreover, even intradermal injection of 100-μM citrusinine-II (50 μl/site) did not alter the locomotor distance of mice models. These results indicate that citrusinine-II is a safe molecule *in vivo*.

3.6 | Citrusinine-II attenuates histamine-induced scratching behaviour

Classically, histamine is the most studied pruritogen associated with itch (Sun & Dong, 2016). To further assess the anti-pruritus effect of citrusinine-II, the histamine-induced scratching model was used. We adopted pretreatment with saline or citrusinine-II by intradermal injection on the nape of the mice before injection of histamine (100 μM). Compared with saline group, injection of histamine significantly increased the spontaneous scratching bouts (Figure 4f). As shown in Figure 4g, after intradermal injection with histamine, the number of spontaneous scratching bouts increased to 64.8 ± 12.6 (n = 6), while that in the negative control group was 13.7 ± 0.6 (n = 6) within 30 min. In contrast, citrusinine-II dose-dependently inhibited the histamine-induced itch behaviour (Figure 4f,g). Five- and 10-μM citrusinine-II (50 μl/site) treatment reduced the scratching behaviour to 31.0 ± 4.5 (n = 6) and 12.0 ± 2.2 (n = 6) within 30 min, respectively. In addition, both intradermal and transdermal delivery of citrusinine-II significantly attenuated histamine-induced itch behaviour in rodent mice models in a dose-dependent manner (Figure 4h), which suggests citrusinine-II is a convenient candidate for anti-pruritus treatment in humans. In addition, we also checked the anti-pruritus activity of citrusinine-II on chloroquine-induced pruritus model. As shown in Figure S5, intradermal injection of chloroquine (400 μg/site) elicited scratching behaviour of the injected site, whereas citrusinine-II showed no striking anti-pruritus activity on chloroquine-induced acute itch.

3.7 | Citrusinine-II alleviates pain behaviour in rodent models

Although there is no overwhelming evidence that TRPV3 has a definite role in analgesic therapy, some reports suggest that TRPV3 channel maybe pain-related (Carreno et al., 2012; Huang & Chung, 2013; Park et al., 2016). In addition, hereditary palmoplantar keratoderma, a rare genetic disorder which is partly due to TRPV3 gain-of-function mutation, is also characterized by severe pain and debilitating itch (Peters et al., 2020). Therefore, we tested the analgesic activity of citrusinine-II on several rodent pain models in which pain was induced by formalin, acetic acid or heat.

Intraplantar injection of formalin induced biphasic pain responses, an early nociceptive pain response (phase I, 0–5 min) and a second nociceptive pain response (phase II, 15–30 min). Intraperitoneal injection of citrusinine-II dose-dependently decreased significantly both phase I and phase II responses (Figure 5a). After the injection of formalin, the average licking time of saline injection mice was 76.8 s. Citrusinine-II attenuated phase I pain response by 4.43%, 12.76% and 51.82% at concentrations of 5, 10 and 50 $\mu mol \cdot kg^{-1}$, respectively.

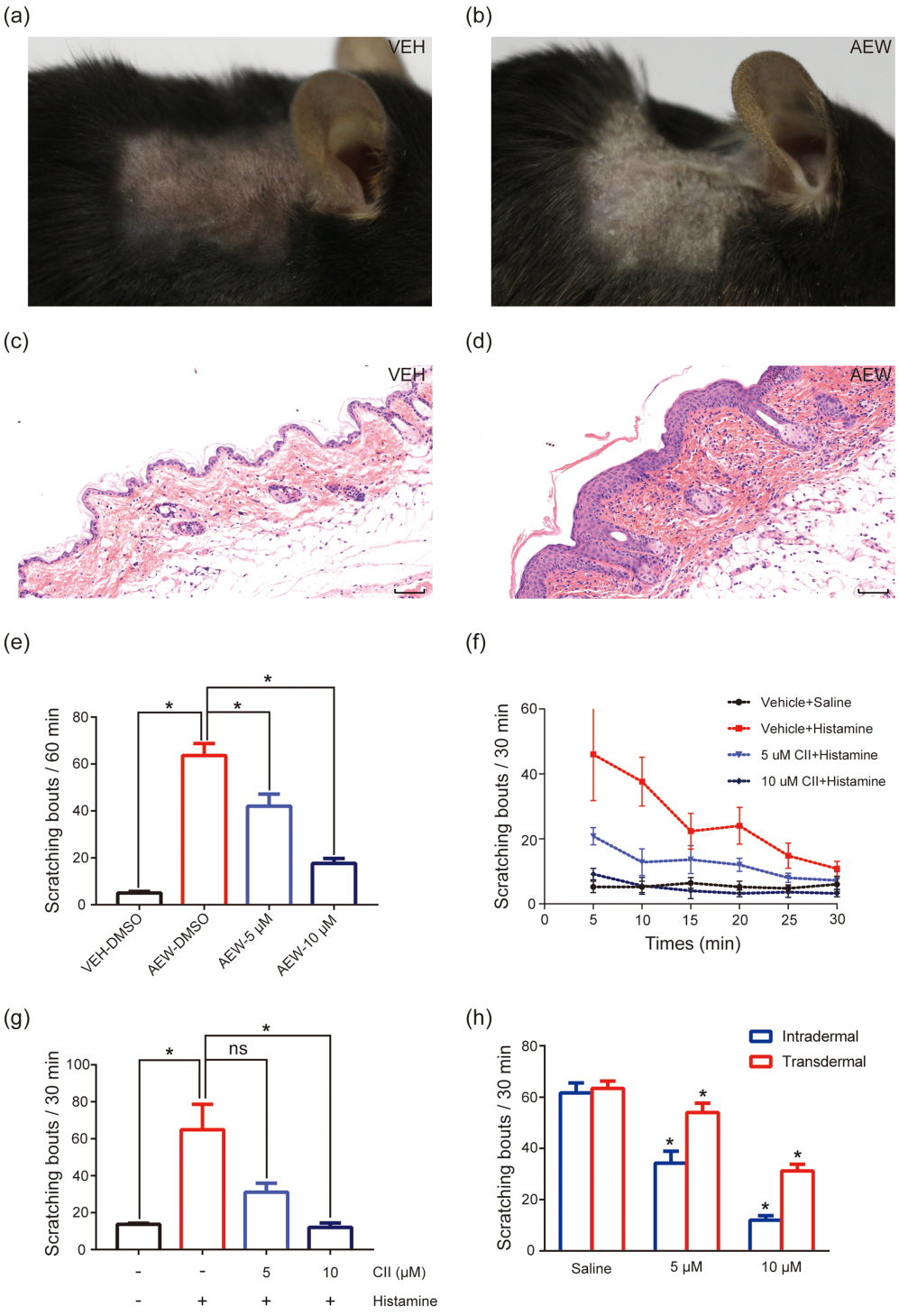

FIGURE 4 Pharmacological inhibition of TRPV3 attenuates acetone-ether-water (AEW) and histamine-induced scratching. (a, b) the illustrative comparison of dry skin in mice treated with water vehicle (VEH) and acetone-ether-water for five consecutive days. (c, d) haematoxylin–eosin staining of nape sections treated with VEH and AEW, respectively. Scale bar = 100 μm. (e) Dose-dependent inhibition of spontaneous scratching bouts pretreated with citrusinine-II in AEW-treated models (n = 5, *P < .05, one-way ANOVA followed by Bonferroni's post hoc test). (f) Time course of nape spontaneous scratching bouts observed in mice after treatment with 50-μl histamine (100 μM), which were pretreatment with vehicle (0.05% DMSO) and citrusinine-II (5 μM and 10 μM, respectively) in 50 μl at the same site. The number of scratching bout was counted every 5 min within 30 min. (g) Dose-dependent inhibition of scratching bouts for the mice pretreated with citrusinine-II (5 μM and 10 μM, respectively) in histamine-induced models (n = 6, *P < .05, Kruskal–Wallis followed by Dunnett's post hoc test). (h) both intradermal and transdermal pretreatment with citrusinine-II dose-dependently inhibited histamine-induced spontaneous scratching (n = 6, *P < .05, two-way ANOVA followed by Sidak's post hoc test)

Citrusinine-II also reduced the nociceptive phase II pain response. At concentrations of 5, 10 and 50 μmol·kg^{-1}, citrusinine-II attenuated the formalin-induced licking time by 4.24%, 22.90% and 58.34%, respectively.

For acetic acid-induced pain behaviour, intraperitoneal injection of citrusinine-II effectively reduced the abdominal writhing movements. At concentrations of 5, 10 and 50 μmol·kg^{-1}, citrusinine-II decreased the acid-induced writhing movements by 22.62%, 42.86%, and 45.24%, respectively (Figure 5b). Citrusinine-II also significantly attenuated heat-induced pain behaviours. In mice subjected to hot plate, citrusinine-II increased withdraw latency time from 5 s for the saline-treated group to 7.8, 10.8 and 13.8 s after intraperitoneal injection with 5, 10 and 50 μmol·kg^{-1} citrusinine-II (Figure 5c). In mice subjected to tail-flick test, citrusinine-II increased withdraw latency time from 3.8 s of the control group to 5.2, 9.2 and 14 s after treated with 5, 10 and 50 μmol·kg^{-1} citrusinine-II, respectively (Figure 5d). All the results suggest that citrusinine-II has good analgesic effect on various somatic and visceral pain models.

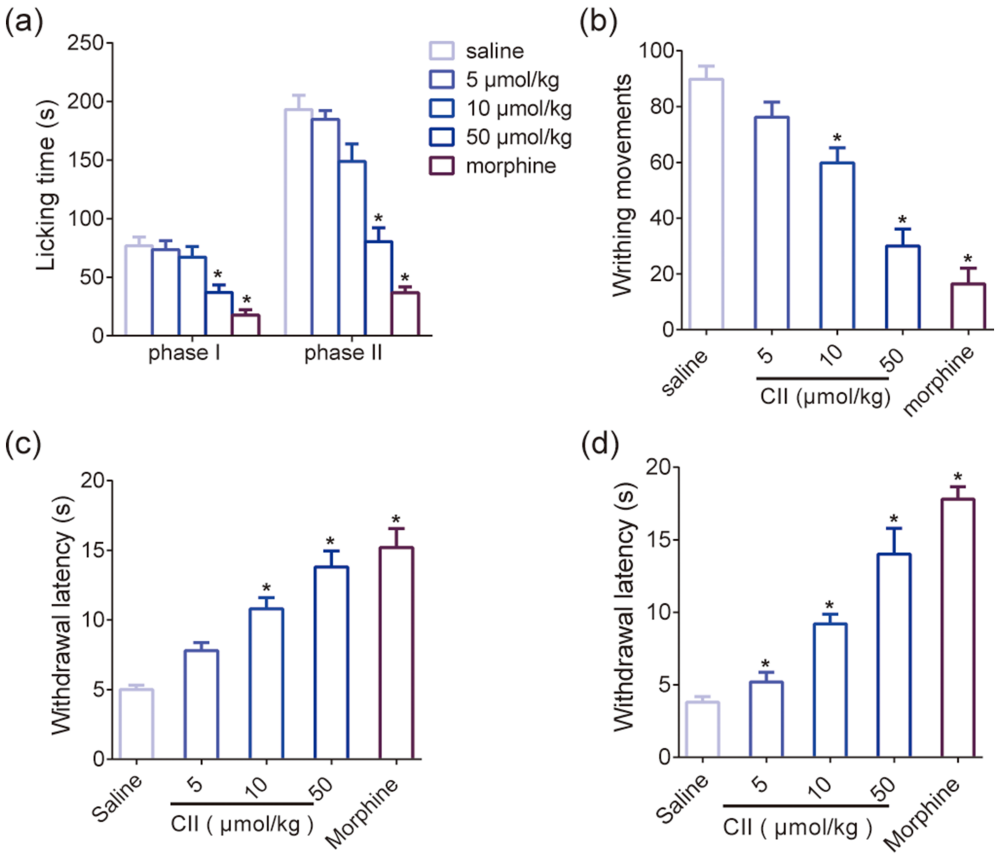

FIGURE 5 Analgesic efficacy of citrusinine-II on mice. (a) Citrusinine-II dose-dependently (5, 10 and 50 μmol·kg^{-1}, respectively) attenuates nociceptive behaviour (paw licking) during phase I (0–5 min post-injection) and phase II (5–15 min post-injection) following intraplantar injection of formalin (n = 5). Positive control, morphine, 100 nmol·kg^{-1}. (b) Citrusinine-II dose-dependently attenuates acetic acid-induced pain behaviour (n = 5). CII, citrusinine-II. Citrusinine-II dose-dependently increased the withdraw latency in hot plate pain models (c) and tail-flick pain models (d). n = 5 each, *P < .05. One-way ANOVA followed by Bonferroni's post hoc test. CII, citrusinine-II

4 | DISCUSSION

Skin is the largest organ of the body which serves from barrier formation to somatic perception (Gravitz, 2018). Keratinocytes, the most abundant cell type in the epidermis, are located at the interface between the external environment and the internal milieu of the body (Huang et al., 2008). Recent works have demonstrated that keratinocytes are required for the behavioural and cellular mechanosensitivity, normal cold and heat sensation, and itch sensitization (Baumbauer et al., 2015; Moehring et al., 2018; Sadler et al., 2020; Szollosi et al., 2019). Keratinocytes can modulate and directly initiate nociceptive responses by eliciting action potential firing in nociceptive as well as tactile sensory afferents (Baumbauer et al., 2015).

TRPV3 ion channel is abundantly expressed in the epidermal keratinocytes. Compelling evidence indicates that TRPV3 channel plays an essential role in itch and pain-related pathological processes. Spontaneous gain-of-function mutations of *Trpv3* gene (Glycine^{573} substituted Serine in DS-*Nh* mice and Glycine^{573} substituted Cysteine in WBN/Kob-Ht rats) elicited severe itching (Asakawa et al., 2006; Yoshioka et al., 2009). Transgenic mice expressing the G573S mutant of TRPV3 channel in keratinocytes caused spontaneous dermatitis and scratching behaviours (Yoshioka et al., 2009). Olmsted syndrome, a hereditary cutaneous disease, is characterized by mutilating palmoplantar keratoderma, periorificial keratotic plaques and severe itching. Intriguingly, an identical gain-of-function missense mutation of TRPV3 channel was found in Olmsted syndrome (Lai-Cheong et al., 2012). In addition, inhibition of TRPV3 channel or knockout *Trpv3* gene significantly attenuated atopic dermatitis-induced scratching behaviours (Qu et al., 2019).

In addition, transgenic mice overexpressing TRPV3 channel showed high sensitivity to noxious heat relative to their wild-type littermates, indicating keratinocyte participation in thermal pain transduction through TRPV3 channels (Huang et al., 2008). **Farnesyl pyrophosphate**, an endogenous algogenic producing molecule, increased nocifensive behaviours in mice with an inflamed hind paw by specifically activating TRPV3 channels (Bang, Yoo, Yang, Cho, & Hwang, 2010). TRPV3 inhibitors, such as **isopentenyl pyrophosphate** and **resolvin D1**, specifically inhibit TRPV3 channels leading to peripheral antinociception (Bang et al., 2011, 2012; Bang, Yoo, Yang, Cho, Kim, & Hwang, 2010). This combined evidence demonstrates that the TRPV3 channel is involved in the pathological process involved in pruritus and pain.

Using a combination of calcium fluorescent assay and whole-cell patch clamp recordings, we identified citrusinine-II compound as a potent inhibitor of TRPV3 channel. At the concentration of 50 μM, citrusinine-II entirely inhibited the current of TRPV3 channel. Furthermore, citrusinine-II is a selective inhibitor of TRPV3 channels as it had no inhibitory activity on other itch-related channels such as ASIC3, P2X3, $Na_v1.7$, $Na_v1.8$ and TRP channels including TRPV1, TRPV4, TRPA1 and TRPM8. Our findings show that citrusinine-II is a potent and selective *in vitro* blocker of TRPV3 channel.

In order to detect the *in vivo* effect of citrusinine-II, we used both acute and chronic itch mice models. Our results showed that citrusinine-II has an anti-pruritic activity as it dose-dependently attenuated the acetone-ether-water-induced chronic scratching behaviours (Figure 4e). Moreover, citrusinine-II nearly completely inhibited histamine-induced scratching bouts within 30 min (Figure 4f,g). Citrusinine-II also proved to be an effective analgesic in rodent mice models, especially heat and acid-induced pain (Figure 5). Since TRPV3 is not functionally expressed in nociceptors (Peier et al., 2002), the inhibitory effect of citrusinine-II was checked on small (<30 μM) dorsal root ganglia neurons. We found that 50-μM citrusinine-II significantly decreased the action potential firing rate by 68.72 ± 2.33% (Figure S6), indicating that citrusinine-II might also target other receptors to affect the neuronal excitability. Moreover, since TRPV3 modulates nociceptive signalling through receptors in the periphery and brain (McGaraughty et al., 2017), we investigated the blood–brain barrier permeability of citrusinine-II in mice using LC–MS/MS detection (Figure S7). Our results revealed that citrusinine-II could cross the blood–brain barrier and therefore citrusinine-II might be involved in the regulation of the descending pain pathway. These findings suggest that citrusinine-II is a valuable candidate drug for the treatment of pruritus-related diseases and that TRPV3 channel is a promising therapeutic target for treating severe itching and pain, as clinically reported in palmoplantar keratoderma and Olmsted syndrome (Choi et al., 2018; Peters et al., 2020).

In summary, our results show that citrusinine-II, a natural acridone alkaloid from *A. monophylla*, is a potent and selective antagonist of TRPV3 channel that plays pivotal role in itch pathophysiology. Citrusinine-II showed excellent anti-pruritus effect both *in vivo* and *in vitro* with little side effects. Our results also indicate the potential of citrusinine-II targeted therapy for pruritus, pain and other skin complaints.

ACKNOWLEDGEMENTS

We would like to thank Prof. Shilong Yang from Northeast Forestry University for valuable comments. This work was supported by the Ministry of Science and Technology of China (2018YFA0801403), the National Natural Science Foundation of China (31930015 and 21761142002), Chinese Academy of Science (XDB31000000, KFJ-STS-SCYD-304, ZSTH-034 and KC Wong Education Foundation) and Science and Technology Department of Yunnan Province (2019ZF003, 2019-YT-053 and 202003 AD150008) to R.L. and from the National Natural Science Foundation of China grants (31900332), Chinese Academy of Sciences (Youth Innovation Promotion Association and "Light of West China" Program) and Science and Technology Department of Yunnan Province (202001AT070121 and 202001AW 070015) to L.L.

AUTHOR CONTRIBUTIONS

Y.H., C.B., L.L. and R.L. designed the experiments. Y.H., A.L., P.K., P.T. and J. H conducted the experiments. Y.H. analysed the data. L.L., Y.H. and P.K. drafted the manuscript, which was revised by all authors who approved the final version.

CONFLICT OF INTEREST

The authors declare no conflicts of interest.

DECLARATION OF TRANSPARENCY AND SCIENTIFIC RIGOUR

This Declaration acknowledges that this paper adheres to the principles for transparent reporting and scientific rigour of preclinical research as stated in the BJP guidelines for Natural Products Research, Design and Analysis, Immunoblotting and Immunochemistry, and Animal Experimentation and as recommended by funding agencies, publishers and other organisations engaged with supporting research.

DATA AVAILABILITY STATEMENT

The data that support the findings of this study are available from the corresponding author upon reasonable request. Some data may not be made available because of privacy or ethical restrictions.

REFERENCES

Alexander, S. P. H., Mathie, A., Peters, J. A., Veale, E. L., Striessnig, J., Kelly, E., Armstrong, J. F., Faccenda, E., Harding, S. D., Pawson, A. J., Sharman, J. L., Southan, C., Davies, J. A., & Collaborators, C. (2019). The concise guide to pharmacology 2019/20: Ion channels. *British Journal of Pharmacology*, *176*(Suppl 1), S142–S228. https://doi.org/10.1111/bph.14749

Asakawa, M., Yoshioka, T., Matsutani, T., Hikita, I., Suzuki, M., Oshima, I., Tsukahara, K., Arimura, A., Horikawa, T., Hirasawa, T., & Sakata, T. (2006). Association of a mutation in TRPV3 with defective hair growth in rodents. *The Journal of Investigative Dermatology*, *126*(12), 2664–2672. https://doi.org/10.1038/sj.jid.5700468

Bang, S., Yoo, S., Yang, T. J., Cho, H., & Hwang, S. W. (2010). Farnesyl pyrophosphate is a novel pain-producing molecule via specific activation of TRPV3. *The Journal of Biological Chemistry*, *285*(25), 19362–19371. https://doi.org/10.1074/jbc.M109.087742

Bang, S., Yoo, S., Yang, T. J., Cho, H., & Hwang, S. W. (2011). Isopentenyl pyrophosphate is a novel antinociceptive substance that inhibits TRPV3 and TRPA1 ion channels. *Pain*, *152*(5), 1156–1164. https://doi.org/10.1016/j.pain.2011.01.044

Bang, S., Yoo, S., Yang, T. J., Cho, H., & Hwang, S. W. (2012). 17(R)-resolvin D1 specifically inhibits transient receptor potential ion channel vanilloid 3 leading to peripheral antinociception. *British Journal of Pharmacology*, *165*(3), 683–692. https://doi.org/10.1111/j.1476-5381.2011.01568.x

Bang, S., Yoo, S., Yang, T. J., Cho, H., Kim, Y. G., & Hwang, S. W. (2010). Resolvin D1 attenuates activation of sensory transient receptor potential channels leading to multiple anti-nociception. *British Journal of Pharmacology*, *161*(3), 707–720. https://doi.org/10.1111/j.1476-5381.2010.00909.x

Baumbauer, K. M., DeBerry, J. J., Adelman, P. C., Miller, R. H., Hachisuka, J., Lee, K. H., Ross, S. E., Koerber, H. R., Davis, B. M., & Albers, K. M. (2015). Keratinocytes can modulate and directly initiate nociceptive responses. *eLife*, *4*. https://doi.org/10.7554/eLife.09674

Carreno, O., Corominas, R., Fernandez-Morales, J., Camina, M., Sobrido, M. J., Fernandez-Fernandez, J. M., Camiña, M., Sobrido, M.-J., Fernández-Fernández, J. M., Pozo-Rosich, P., Cormand, B., & Macaya, A. (2012). SNP variants within the vanilloid TRPV1 and TRPV3 receptor genes are associated with migraine in the Spanish population. *American Journal of Medical Genetics. Part B, Neuropsychiatric Genetics*, *159B*(1), 94–103. https://doi.org/10.1002/ajmg.b.32007

Choi, J. Y., Kim, S. E., Lee, S. E., & Kim, S. C. (2018). Olmsted syndrome caused by a heterozygous p.Gly568Val missense mutation in TRPV3 gene. *Yonsei Medical Journal*, *59*(2), 341–344. https://doi.org/10.3349/ymj.2018.59.2.341

Chung, M. K., Guler, A. D., & Caterina, M. J. (2005). Biphasic currents evoked by chemical or thermal activation of the heat-gated ion channel, TRPV3. *The Journal of Biological Chemistry*, *280*(16), 15928–15941. https://doi.org/10.1074/jbc.M500596200

Colton, C. K., & Zhu, M. X. (2007). 2-Aminoethoxydiphenyl borate as a common activator of TRPV1, TRPV2, and TRPV3 channels. *Handbook of Experimental Pharmacology*, (179), 173–187. https://doi.org/10.1007/978-3-540-34891-7_10

Curtis, M. J., Alexander, S., Cirino, G., Docherty, J. R., George, C. H., Giembycz, M. A., Hoyer, D., Insel, P. A., Izzo, A. A., Ji, Y., MacEwan, D. J., Sobey, C. G., Stanford, S. C., Teixeira, M. M., Wonnacott, S., & Ahluwalia, A. (2018). Experimental design and analysis and their reporting II: Updated and simplified guidance for authors and peer reviewers. *British Journal of Pharmacology*, *175*(7), 987–993. https://doi.org/10.1111/bph.14153

Dalgard, F., Svensson, A., Holm, J. O., & Sundby, J. (2004). Self-reported skin morbidity in Oslo. Associations with sociodemographic factors among adults in a cross-sectional study. *The British Journal of Dermatology*, *151*(2), 452–457. https://doi.org/10.1111/j.1365-2133.2004.06058.x

Devigili, G., Eleopra, R., Pierro, T., Lombardi, R., Rinaldo, S., Lettieri, C., Faber, C. G., Merkies, I. S. J., Waxman, S. G., & Lauria, G. (2014). Paroxysmal itch caused by gain-of-function Nav1.7 mutation. *Pain*, *155*(9), 1702–1707. https://doi.org/10.1016/j.pain.2014.05.006

Duque, M. I., Vogel, C. A., Fleischer, A. B. Jr., & Yosipovitch, G. (2004). Over-the-counter topical antipruritic agents are commonly recommended by office-based physicians: An analysis of US practice patterns. *The Journal of Dermatological Treatment*, *15*(3), 185–188. https://doi.org/10.1080/09546630410027337

Grandl, J., Hu, H., Bandell, M., Bursulaya, B., Schmidt, M., Petrus, M., & Patapoutian, A. (2008). Pore region of TRPV3 ion channel is specifically required for heat activation. *Nature Neuroscience*, *11*(9), 1007–1013. https://doi.org/10.1038/nn.2169

Gravitz, L. (2018). Skin. *Nature*, *563*(7732), S83. https://doi.org/10.1038/d41586-018-07428-4

Han, J. H., Choi, H. K., & Kim, S. J. (2012). Topical TRPM8 agonist (icilin) relieved vulva pruritus originating from lichen sclerosus et atrophicus. *Acta Dermato-Venereologica*, *92*(5), 561–562. https://doi.org/10.2340/00015555-1244

Han, Y., Li, B., Yin, T. T., Xu, C., Ombati, R., Luo, L., Xia, Y., Xu, L., Zheng, J., Zhang, Y., Yang, F., Wang, G.-D., Yang, S., & Lai, R. (2018). Molecular mechanism of the tree shrew's insensitivity to spiciness. *PLoS Biology*, *16*(7), e2004921. https://doi.org/10.1371/journal.pbio.2004921

Huang, S. M., & Chung, M. K. (2013). Targeting TRPV3 for the development of novel analgesics. *The Open Pain Journal*, *6*(Spec Iss 1), 119–126. https://doi.org/10.2174/1876386301306010119

Huang, S. M., Lee, H., Chung, M. K., Park, U., Yu, Y. Y., Bradshaw, H. B., Coulombe, P. A., Walker, J. M., & Caterina, M. J. (2008). Overexpressed transient receptor potential vanilloid 3 ion channels in skin keratinocytes modulate pain sensitivity via prostaglandin E2. *The Journal of Neuroscience: The Official Journal of the Society for Neuroscience*, *28*(51), 13727–13737. https://doi.org/10.1523/jneurosci.5741-07.2008

Izzo, A. A., Teixeira, M., Alexander, S. P., Cirino, G., Docherty, J. R., George, C. H., Insel, P. A., Ji, Y., Kendall, D. A., Panattieri, R. A., Sobey, C. G., Stanford, S. C., Stefanska, B., Stephens, G., & Ahluwalia, A. (2020). A practical guide for transparent reporting of research on natural products in the *British Journal of Pharmacology* : Reproducibility of natural product research. *British Journal of Pharmacology*, *177*(10), 2169–2178. https://doi.org/10.1111/bph.15054

Kuhn, H., Kappes, L., Wolf, K., Gebhardt, L., Neurath, M. F., Reeh, P., Fischer, M. J. M., & Kremer, A. E. (2020). Complementary roles of murine NaV1.7, NaV1.8 and NaV1.9 in acute itch signalling. *Scientific Reports*, *10*(1), 2326. https://doi.org/10.1038/s41598-020-59092-2

Lai-Cheong, J. E., Sethuraman, G., Ramam, M., Stone, K., Simpson, M. A., & McGrath, J. A. (2012). Recurrent heterozygous missense mutation, p.Gly573Ser, in the TRPV3 gene in an Indian boy with sporadic Olmsted syndrome. *The British Journal of Dermatology*, *167*(2), 440–442. https://doi.org/10.1111/j.1365-2133.2012.11115.x

Lilley, E., Stanford, S. C., Kendall, D. E., Alexander, S. P. H., Cirino, G., Docherty, J. R., George, C. H., Insel, P. A., Izzo, A. A., Ji, Y., Panettieri, R. A., Sobey, C. G., Stefanska, B., Stephens, G., Teixeira, M., & Ahluwalia, A. (2020). ARRIVE 2.0 and the *British Journal of Pharmacology*: Updated guidance for 2020. *British Journal of Pharmacology*, *177*(16), 3611–3616. https://doi.org/10.1111/bph.15178

Luo, J., Zhu, Y., Zhu, M. X., & Hu, H. (2011). Cell-based calcium assay for medium to high throughput screening of TRP channel functions using FlexStation 3. *Journal of Visualized Experiments: JoVE*, *3149*(54). https://doi.org/10.3791/3149

Luo, L., Li, B., Wang, S., Wu, F., Wang, X., Liang, P., Ombati, R., Chen, J., Lu, X., Cui, J., Lu, Q., Zhang, L., Zhou, M., Tian, C., Yang, S., & Lai, R. (2018). Centipedes subdue giant prey by blocking KCNQ channels. *Proceedings of the National Academy of Sciences of the United States of America*, *115*(7), 1646–1651. https://doi.org/10.1073/pnas.1714760115

Luo, L., Wang, Y., Li, B., Xu, L., Kamau, P. M., Zheng, J., Yang, F., Yang, S., & Lai, R. (2019). Molecular basis for heat desensitization of TRPV1 ion channels. *Nature Communications*, *10*(1), 2134. https://doi.org/10.1038/s41467-019-09965-6

Matterne, U., Apfelbacher, C. J., Loerbroks, A., Schwarzer, T., Buttner, M., Ofenloch, R., Diepgen, T. L., & Weisshaar, E. (2011). Prevalence, correlates and characteristics of chronic pruritus: A population-based cross-sectional study. *Acta Dermato-Venereologica*, *91*(6), 674–679. https://doi.org/10.2340/00015555-1159

McGaraughty, S., Chu, K. L., Xu, J., Leys, L., Radek, R. J., Dart, M. J., Gomtsyan, A., Schmidt, R. G., Kym, P. R., & Brederson, J. D. (2017). TRPV3 modulates nociceptive signaling through peripheral and supraspinal sites in rats. *Journal of Neurophysiology*, *118*(2), 904–916. https://doi.org/10.1152/jn.00104.2017

Misery, L., Santerre, A., Batardiere, A., Hornez, N., Nedelec, A. S., Le Caer, F., Bourgeois, P., Huet, F., & Neufang, G. (2019). Real-life study of anti-itching effects of a cream containing mentho-xypropanediol, a TRPM8 agonist, in atopic dermatitis patients. *Journal of the European Academy of Dermatology and Venereology*, *33*(2), e67–e69. https://doi.org/10.1111/jdv.15199

Moehring, F., Cowie, A. M., Menzel, A. D., Weyer, A. D., Grzybowski, M., Arzua, T., Geurts, A. M., Palygin, O., & Stucky, C. L. (2018). Keratinocytes mediate innocuous and noxious touch via ATP-P2X4 signaling. *eLife*, *7*. https://doi.org/10.7554/eLife.31684

Nattkemper, L. A., Tey, H. L., Valdes-Rodriguez, R., Lee, H., Mollanazar, N. K., Albornoz, C., Sanders, K. M., & Yosipovitch, G. (2018). The genetics of chronic itch: Gene expression in the skin of patients with atopic dermatitis and psoriasis with severe itch. *The Journal of Investigative Dermatology*, *138*(6), 1311–1317. https://doi.org/10.1016/j.jid.2017.12.029

Park, D. J., Kim, S. H., Nah, S. S., Lee, J. H., Kim, S. K., Lee, Y. A., Kim, S.-K., Lee, Y.-A., Hong, S.-J., Kim, H.-S., Lee, H.-S., Kim, H. A., Joung, C.-I., Kim, S.-H., & Lee, S. S. (2016). Polymorphisms of the TRPV2 and TRPV3 genes associated with fibromyalgia in a Korean population. *Rheumatology (Oxford)*, *55*(8), 1518–1527. https://doi.org/10.1093/rheumatology/kew180

Peier, A. M., Reeve, A. J., Andersson, D. A., Moqrich, A., Earley, T. J., Hergarden, A. C., Story, G. M., Colley, S., Hogenesch, J. B.,

McIntyre, P., Bevan, S., & Patapoutian, A. (2002). A heat-sensitive TRP channel expressed in keratinocytes. *Science*, *296*(5575), 2046–2049. https://doi.org/10.1126/science.1073140

Peng, Z., Li, W. G., Huang, C., Jiang, Y. M., Wang, X., Zhu, M. X., Cheng, X., & Xu, T. L. (2015). ASIC3 mediates itch sensation in response to coincident stimulation by acid and nonproton ligand. *Cell Reports*, *13*(2), 387–398. https://doi.org/10.1016/j.celrep.2015.09.002

Percie du Sert, N., Hurst, V., Ahluwalia, A., Alam, S., Avey, M. T., Baker, M., Browne, W. J., Clark, A., Cuthill, I. C., Dirnagl, U., Emerson, M., Garner, P., Holgate, S. T., Howells, D. W., Karp, N. A., Lazic, S. E., Lidster, K., MacCallum, C. J., Macleod, M., … Würbel, H. (2020). The ARRIVE guidelines 2.0: Updated guidelines for reporting animal research. *PLoS Biology*, *18*(7), e3000410. https://doi.org/10.1371/journal.pbio.3000410

Peters, F., Kopp, J., Fischer, J., & Tantcheva-Poor, I. (2020). Mutation in TRPV3 causes painful focal plantar keratoderma. *Journal of the European Academy of Dermatology and Venereology*. *34*(10), E620–E622. https://doi.org/10.1111/jdv.16498

Qu, Y., Wang, G., Sun, X., & Wang, K. (2019). Inhibition of the warm temperature-activated Ca^{2+}-permeable transient receptor potential Vanilloid TRPV3 channel attenuates atopic dermatitis. *Molecular Pharmacology*, *96*(3), 393–400. https://doi.org/10.1124/mol.119.116962

Sadler, K. E., Moehring, F., & Stucky, C. L. (2020). Keratinocytes contribute to normal cold and heat sensation. *eLife*, *9*. https://doi.org/10.7554/eLife.58625

Shiratori-Hayashi, M., Hasegawa, A., Toyonaga, H., Andoh, T., Nakahara, T., Kido-Nakahara, M., Furue, M., Kuraishi, Y., Inoue, K., Dong, X., & Tsuda, M. (2019). Role of P2X3 receptors in scratching behavior in mouse models. *The Journal of Allergy and Clinical Immunology*, *143*(3), 1252–1254e1258. https://doi.org/10.1016/j.jaci.2018.10.053

Silverberg, J. I. (2017). Selected comorbidities of atopic dermatitis: Atopy, neuropsychiatric, and musculoskeletal disorders. *Clinics in Dermatology*, *35*(4), 360–366. https://doi.org/10.1016/j.clindermatol.2017.03.008

Singh, A. K., McGoldrick, L. L., & Sobolevsky, A. I. (2018). Structure and gating mechanism of the transient receptor potential channel TRPV3. *Nature Structural & Molecular Biology*, *25*(9), 805–813. https://doi.org/10.1038/s41594-018-0108-7

Song, J., Xian, D., Yang, L., Xiong, X., Lai, R., & Zhong, J. (2018). Pruritus: Progress toward pathogenesis and treatment. *BioMed Research International*, *2018*(12), 9625936. https://doi.org/10.1155/2018/9625936

Spyra, S., Meisner, A., Schaefer, M., & Hill, K. (2017). COX-2-selective inhibitors celecoxib and deracoxib modulate transient receptor potential vanilloid 3 channels. *British Journal of Pharmacology*, *174*(16), 2696–2705. https://doi.org/10.1111/bph.13893

Stander, S., Weisshaar, E., Mettang, T., Szepietowski, J. C., Carstens, E., Ikoma, A., Bergasa, N. V., Gieler, U., Misery, L., Wallengren, J., Darsow, U., Streit, M., Metze, D., Luger, T. A., Greaves, M. W., Schmelz, M., Yosipovitch, G., & Bernhard, J. D. (2007). Clinical classification of itch: A position paper of the international forum for the study of itch. *Acta Dermato-Venereologica*, *87*(4), 291–294. https://doi.org/10.2340/00015555-0305

Sun, S., & Dong, X. (2016). Trp channels and itch. *Seminars in Immunopathology*, *38*(3), 293–307. https://doi.org/10.1007/s00281-015-0530-4

Sun, X. Y., Sun, L. L., Qi, H., Gao, Q., Wang, G. X., Wei, N. N., & Wang, K. (2018). Antipruritic effect of natural coumarin osthole through selective inhibition of Thermosensitive TRPV3 channel in the skin. *Molecular Pharmacology*, *94*(4), 1164–1173. https://doi.org/10.1124/mol.118.112466

Szollosi, A. G., McDonald, I., Szabo, I. L., Meng, J., van den Bogaard, E., & Steinhoff, M. (2019). TLR3 in chronic human itch: A keratinocyte-associated mechanism of peripheral itch sensitization. *The Journal of Investigative Dermatology*, *139*(11), 2393–2396e2396. https://doi.org/10.1016/j.jid.2019.04.018

Wang, G., & Wang, K. (2017). The ca(2+)-permeable cation transient receptor potential TRPV3 channel: An emerging pivotal target for itch and skin diseases. *Molecular Pharmacology*, *92*(3), 193–200. https://doi.org/10.1124/mol.116.107946

Wei, L., Dong, L., Zhao, T., You, D., Liu, R., Liu, H., Liu, H., Yang, H., & Lai, R. (2011). Analgesic and anti-inflammatory effects of the amphibian neurotoxin, anntoxin. *Biochimie*, *93*(6), 995–1000. https://doi.org/10.1016/j.biochi.2011.02.010

Xu, L., Han, Y., Chen, X., Aierken, A., Wen, H., Zheng, W., Wang, H., Lu, X., Zhao, Z., Ma, C., Liang, P., Yang, W., Yang, S., & Yang, F. (2020). Molecular mechanisms underlying menthol binding and activation of TRPM8 ion channel. *Nature Communications*, *11*(1), 3790–3790. https://doi.org/10.1038/s41467-020-17582-x

Yamamoto-Kasai, E., Imura, K., Yasui, K., Shichijou, M., Oshima, I., Hirasawa, T., Sakata, T., & Yoshioka, T. (2012). TRPV3 as a therapeutic target for itch. *The Journal of Investigative Dermatology*, *132*(8), 2109–2112. https://doi.org/10.1038/jid.2012.97

Yang, S., Xiao, Y., Kang, D., Liu, J., Li, Y., Undheim, E. A., Klint, J. K., Rong, M., Lai, R., & King, G. F. (2013). Discovery of a selective NaV1.7 inhibitor from centipede venom with analgesic efficacy exceeding morphine in rodent pain models. *Proceedings of the National Academy of Sciences of the United States of America*, *110*(43), 17534–17539. https://doi.org/10.1073/pnas.1306285110

Yoshioka, T., Imura, K., Asakawa, M., Suzuki, M., Oshima, I., Hirasawa, T., Sakata, T., Horikawa, T., & Arimura, A. (2009). Impact of the Gly573Ser substitution in TRPV3 on the development of allergic and pruritic dermatitis in mice. *The Journal of Investigative Dermatology*, *129*(3), 714–722. https://doi.org/10.1038/jid.2008.245

Zhang, H., Sun, X., Qi, H., Ma, Q., Zhou, Q., Wang, W., & Wang, K. (2019). Pharmacological inhibition of the temperature-sensitive and Ca^{2+}-permeable transient receptor potential vanilloid TRPV3 channel by natural forsythoside B attenuates pruritus and cytotoxicity of keratinocytes. *The Journal of Pharmacology and Experimental Therapeutics*, *368*(1), 21–31. https://doi.org/10.1124/jpet.118.254045

SUPPORTING INFORMATION

Additional supporting information may be found online in the Supporting Information section at the end of this article.

How to cite this article: Han Y, Luo A, Kamau PM, et al. A plant-derived TRPV3 inhibitor suppresses pain and itch. *Br J Pharmacol*. 2021;178:1669–1683. https://doi.org/10.1111/bph.15390